Spectroscopic study of Methylbenzyl radicals in a corona excited supersonic expansion

Chang soon Huh

Abstract— **We report the spectroscopic and *ab initio* and spectroscopic evidence of the 1, 3, 5- trimethylbenzyl and 3, 5-dimethylbenzyl radical in corona excited supersonic expansion(CESE). The electronically hot but jet-cooled 1, 3, 5- trimethylbenzyl and 3, 5-dimethylbenzyl radical has been produced from precursor 1, 2, 3-trimethylbenzene seeded in large amount inert carrier gas helium by using the technique of CESE with a pinhole-type glass nozzle. *AB initio* calculation were carried out with the GAUSSIAN-09 package and vibronic emission spectrum of the 3,5-dimethylbenzyl radicals were recorded with a long path monochromator in the $D_1 \rightarrow D_0$ electronic transition in the visible region. *Ab initio* calculation of the ground-state benzyl radical have been carried out with density functional method and the complete basis set model. The observed spectrum is consistent with the result of vibrational frequencies of the *ab initio* calculation and the benzyl radical ground state reaction mechanism through the hydrogen migration is presented. Furthermore, the *ab initio* calculation explains the benzyl radical generation mechanism in the excited state through the anti-bonding energy surface.**

***Index Terms*— Methylbenzyl radical, Corona Excited Supersonic Expansion(CESE), Vibronic Emission Spectrum, *Ab initio* Calculation**

I. INTRODUCTION

While benzyl radical, a prototype of aromatic radical, has attracted much attention from spectroscopists, alkyl substituted benzyl radicals have been less studied as large aromatic radicals [1,2]. The earlier works of the xylyl radicals in the visible region were reported by Schuler et al. [3] and by Walker and Barrow [4]. Bindley et al. [5,6] made vibronic assignments of the bands from analysis of the emission spectra of xylyl radicals produced by an electric discharge of the xylenes.[7]

Charlton and Thrush [8] have observed the laser induced fluorescence (LIF) spectra of alkyl substituted benzyl radicals and have measured the lifetime in the excited vibronic states. Recently, our molecular spectroscopy group[9-12] have extended the assignments of vibrational modes of xylyl radicals from the vibronic emission spectra. The controversial assignments of p-xylyl radicals have been confirmed by the bandshape analysis of the vibronic bands from high resolution emission spectra [12]. The torsional barrier of the internal methyl group has been calculated for the xylyl radicals by Lin and Miller [13] from an analysis of the laser induced fluorescence excitation and dispersed emission spectra. Although the exact mechanism for generation and excitation of benzyl-type radicals in a corona discharge is not known, the analysis of vibronic spectrum observed provides the species produced with the spectroscopic evidence for identification.

Supersonic jet expansion has been recognized as a powerful spectroscopic technique for observing molecular spectra in the gas phase [14]. The spectral simplification and transient molecular stabilization associated with expansion of inert carrier gas cannot be achieved in any other ways. Combination of technique of supersonic jet expansion with emission spectroscopy has had an enormous impact on the repertoire of spectroscopic studies of transient molecular species. Of the emission sources utilizing these combinations, the one providing enough continuous photon intensity for high resolution studies of weak transition is the pinhole-type glass nozzle [15,16] which has been widely employed for observation of the vibronic emission spectra of transient species [17]. This has been applied to the observation of the vibronic emission spectra of many jet-cooled benzyl-type radicals in the gas phase [18-21].

In this work, we report the benzyl-type radicals generated in a corona discharge from teramethylbenzene and trimethylbenzene and provide the first spectroscopic evidence of the $D_1 \rightarrow D_0$ electronic transition of trimethylbenzyl radical and dimethylbenzyl radical and their vibrational mode frequencies in the ground electronic state have been determined by comparison with an ab initio calculation and the known vibrational mode frequencies of the precursor.

II. EXPERIMENTAL DETAILS

The Figure 1 shows the schematic diagram of the corona excited supersonic jet system used in this work, which is mainly divided into three parts; (a) energy source, (b) electric discharge and supersonic system and (c) spectrometer and acquisition system. For the generation of transient molecules in a jet from the precursor molecules, we have employed a conventional corona discharge system which is similar to that developed by Engelking [14]. A conventional corona discharge [22] coupled with a supersonic expansion is consisted of a thin metal rod, terminated with a sharp point, mounted inside an insulating and inert tube. Forming a supersonic nozzle. The metal tip is placed very close to the exit hole and a high positive voltage is applied to the rod. Thus, the nozzle body, in this work, was formed from a thick-walled quartz tube of 12㎜ outer diameter, 2㎜ thickness, and 250㎜ length, narrowed by flame heating at one end to a capillary of the desired pinhole size. The nozzle was connected to threaded adaptor (Ace glass model 5027-05). A long and sharpened anode, made of a 1.6㎜ diameter stainless steel rod was inserted through a rubber o-ring into the quartz nozzle for the generation and excitation of transient molecules. The o-ring was tightened by a teflon bushing with a hole in center through which the anode was connected to the high voltage electric dc power supply (Bertan model 210-05R).

The position of the metal tip used for the anode has been proven to be critical for the stability of the discharge over a long period. For example, in Engelking type corona discharge the metal tip is located inside the nozzle and the molecules are excited before expansion, which substantially reduces the stability of the discharge when heavy organic compounds are used as precursors, the messy fragments generated by an electric discharge of the organic precursor easily block the narrow hole of the nozzle. Thus, in this design we put the metal tip outside the nozzle. Even though the length of the metal tip exposed outside the nozzle is less than 0.5㎜, it changes the mechanism, leading to excitation after expansion. However, it is very important to let the metal tip be centered at the hole for the straightly downstream beam. The anode was firmly fixed into the center of nozzle by using teflon holders inside the nozzle. The teflon holder made of 3㎜ thickness of teflon disk of whose diameter is exactly same as the inner diameter of the nozzle has a center hole for the anode and several small holes for the gas flow. The nozzle was positioned into the expansion chamber via a Cajon fit attached to the stainless steel flange. The cathode was located at under the chamber supporter made by an acrylic plate to avoid seeing the arching by the spectrometer during the discharge. The arching was more severe when the surface of the cathode was contaminated by foreign compounds.

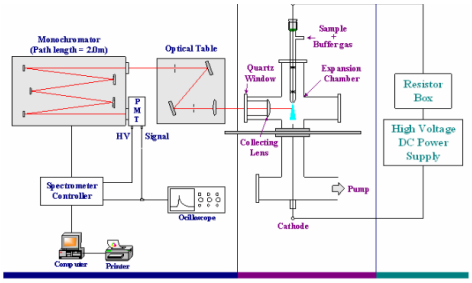

Figure. 1. The schematic diagram of the CESE system.

When a dilute mixture of a precursor molecule in a rare gas was expanded through the orifice, an electrical discharge produced not only molecular fragments but also vibronically excited molecules. The details of the nozzle system is shown in Figure 2. The anode was connected via a 200kΩ ballast resister to the high voltage electric dc power supply which has a maximum 5kV and 40㎃ capacity. The expansion gas is supplied from 2 atm rare gas reservoir seeded with a small quantity of stable precursor molecules vaporized inside the vaporizing vessel. The concentration of the precursor in a carrier gas can be controlled by immersing the sample in a temperature-controllable water bath. Since the discharge occurs in the high pressure region of the nozzle, molecules undergo collisional relaxation into the vibrational ground level of the electronic excited state before they emit. Thus, it has an advantage of observing the transitions from a single vibronic state.

For the rotational cooling, the supersonic expansion chamber was made of six-way cross pyrex tube of 50㎜ inner diameter. The chamber was evacuated by a 800L/min mechanical vacuum pump (WS Automa model W2V80), resulting in the pressure range of 1.5-1.8 Torr during the operation with 2.0 atm of backing pressure. The emitting light from the downstream jet was collected through a collecting quartz lens of 38㎜ diameter and 50㎜ focal length placed at focal length from the tip of the nozzle, and focused onto the slit of the double-type monochromator using a combination of two mirrors and a lens.

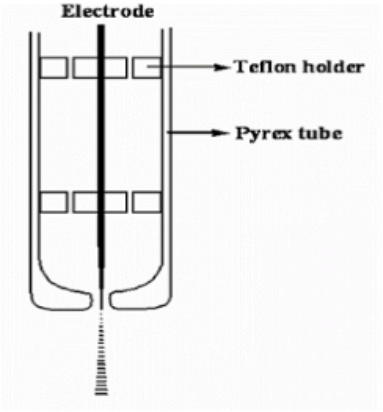

Figure. 2. The details of the nozzle structure.

For the spectrometer, we have employed the double type monochromator (Jobin Yvon model U-1000) which has effective path length of 2.0m using 3 mirrors and 2 gratings of 1800 groves/㎜. The scanning range of the spectrometer is from 11,500 cm^{-1} to 32,000 cm^{-1}, with a maximum resolving power of 0.15 cm^{-1} at 17,000 cm^{-1} which is good enough to observe the rotational contour of the vibronic band of large molecules in a jet. For the photon counting, a head-on photomultiplier tube (Hamamatsu model R649) was employed. The output of the PMT was fed to the spectrometer control box via the preamplifier. The spectrometer was fully operated using a software SPECTRAMAX [23] by a personal computer.

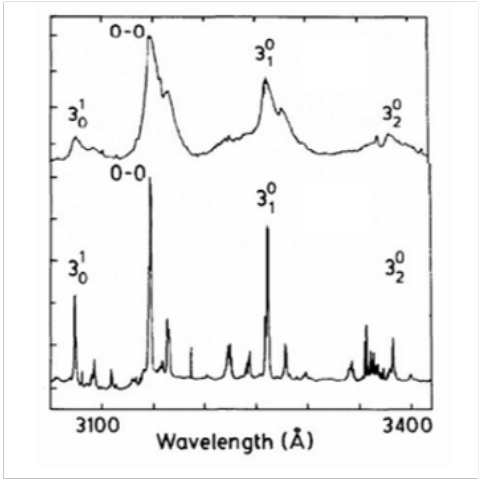

Comparison of spectrum bandshape of transition with nozzle (below) and without nozzle (above).

The methyl-substituted toluene of the reagent grade was obtained commercially from Aldrich and used without further purification. For the CESE experiment, the electronically excited methyl-substituted benzyl radical was generated from methyl-substituted toluene by corona

discharge in a supersonic expansion with helium buffer gas. The methyl-substituted toluene was vaporized at room temperature inside the vaporizing vessel made of thick Pyrex glass bottle under 2.0 atm of He gas. The concentration of the precursor in the carrier gas was adjusted for the maximum emission intensity and believed to be about 1% in the gas mixture.

The discharge condition was 5 ㎃ at the 2.0 ㎸ dc potential. A blue colored jet was the evidence of existence of the methyl-substituted benzyl radical in the jet. The light emanating from the downstream jet area 5 ㎜ away from the nozzle opening was collimated by a quartz lens placed inside the expansion chamber and focused onto the slit of the monochromator (Jobin Yvon U1000) employing two 1800 lines/㎜ gratings, and detected with a cooled photomultiplier tube (Hamamatsu R649) and a photon counting system. During the scans, the slits were set to 0.200 ㎜, providing resolution of 1 cm^{-1} at the visible region.

The spectral region from 18000 to 22000 $cm^{-1}$was scanned in about 1 hr in 2.0 cm^{-1} steps to obtain the final spectrum. The frequency of the spectrum was calibrated using th He atomic lines observed at the same frequency region as the methyl-substituted benzyl radical and is believed to be accurate within ±0.2 cm^{-1}.

Since the precursor and methyl-substituted benzyl radical have many vibrational modes and the assignments have not been completed, we performed to assist assignment of their spectrum. *Ab initio* calculations were carried out using the GAUSSIAN 09 for Windows package. Geometry optimizations were performed at the RHF and B3LYP method for the methyl-substituted toluene and also UHF and B3LYP method for the methyl-substituted benzyl radical. The calculations were executed with a personal computer equipped with an Intel Pentium VI, 3 GHz processor and 2 GMB RAM.

III. RESULTS AND DISCUSSION

The The general electronic structure of the benzyl-type radical can be simply described by the Huckel theory. The seven π-molecular orbitals can be written in terms of the seven *p*-atomic orbitals. For the π-electron system, there exist single nonbonding orbital and pairs of bonding and antibonding orbitals located with equal energy differences below and above the nonbonding orbitals. The seven molecular orbitals of benzyl-type radical would give rise to the following ground-state configuration in C_{2v} symmetry.

$$(1b_2)^2\,(1b_2)^2\,(2a_2)^2\,(3b_2)^1\,(4a_2)\,(2b_2)\,(5b_2) \Rightarrow 1\,^2B_2$$

The lowest three orbitals are bonding, the $3b_2$ orbital nonbonding, and the three highest orbitals antibonding with the based upon the pairing theorem, for excited electronic states, there are two possible isoenergetic ways of promoting an electron involving a_2 MOs, resulting in two electron configurations of A_2 symmetry.

$$(a)\ (1b_2)^2\,(1b_2)^2\,(2a_2)^1\,(3b_2)^2\,(4a_2)\,(2b_2)\,(5b_2) \Rightarrow {}^2A_2$$
$$(b)\ (1b_2)^2\,(1b_2)^2\,(2a_2)^2\,(3b_2)\,(4a_2)^1\,(2b_2)\,(5b_2) \Rightarrow {}^2A_2$$

These two promoting ways are shown as paths (a) and (b). Similarly, there are also two isoenergetic one-electron promotions as paths (c) and (d) involving b_2 MOs. These give rise to two electron configurations of B_2 symmetry in Figure 4. [24]

$$(c)\ (1b_2)^2\,(1b_2)^1\,(2a_2)^2\,(3b_2)^2\,(4a_2)\,(2b_2)\,(5b_2) \Rightarrow {}^2B_2$$
$$(d)\ (1b_2)^2\,(1b_2)^2\,(2a_2)^2\,(3b_2)\,(4a_2)\,(2b_2)^1\,(5b_2) \Rightarrow {}^2B_2$$

There is also the excited configuration

$$(1b_2)^2\,(1b_2)^2\,(2a_2)^1\,(3b_2)^1\,(4a_2)^1\,(2b_2)\,(5b_2) \Rightarrow {}^4B_2,\ {}^2B_2,\ {}^2B_2$$

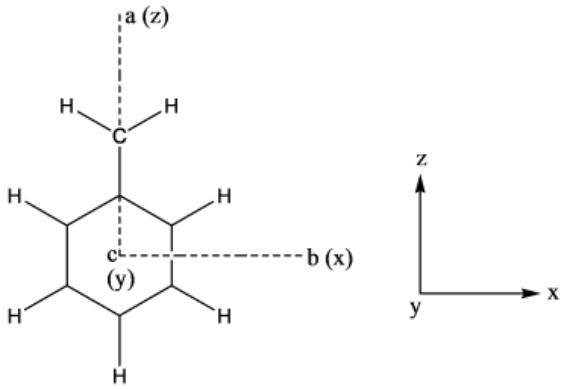

Figure. 3. Molecular fixed-axis system of benzyl radical.

In the one-electron approximation, we would have as the lowest excited electronic states a degenerate pair of $^2A_2$ states with another degenerate pair of $^2B_2$ states only slightly higher in energy. However, in the presence of configuration interaction (CI), the two degenerate pairs of zeroth order electronic states of the same symmetry interact and repel very strongly, splitting widely the initially degenerate pairs. In the case of the $^2B_2$ states the lower frequency state, i.e. 2^2B_2, is the antisymmetric linear combination of mixed state and carries a small oscillator strength, due to cancellation of transition moments calculated from the single configurations [25]. For the same reason, the lower of the $^2A_2$ states,i.e. 1^2A_2, lies in the same energy region and also has a low oscillator strength.

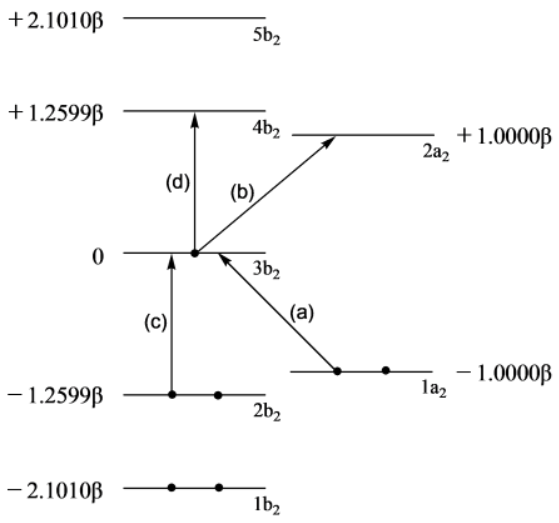

Figure 4. Huckel molecular orbital energy level scheme of benzyl radical.

□.1 *Ab initio* calculation of 1,3,5-trimethylbenzene

It *Ab initio* calculations also were carried out with the GAUSSIAN-09 package. Geometry optimizations were performed at the HF and B3LYP method and basis set; 6-31G*, 6-311G*, 6-311G(df,pd), cc-pvdz. Optimized geometries were subsequently used for the calculations of the frequencies and the shapes of the respective normal modes.

In the *ab initio* calculations, it is compared with each method and basis set using 1,3,5-trimethylbenzene. It is best optimization to use B3LYP/cc-pvdz. The comparison of method of 1,3,5-trimethylbenzene calculation with experiment is given in Table 1.

The calculated frequencies of 1,3,5-trimethylbenzene matched the experimental ones and B3LYP method for vibration assignment is better than HF method. The results of calculation are given in Table 9.

Table 1. Bond length comparison of calculation with experimental data of 1,3,5-trimethylbenzene.

B3LYP/6-31g*	-350.202451	1.5125	1.3995
B3LYP/6-311g*	-350.2734021	1.5105	1.3975
B3LYP/6-31g(df,pd)	-350.305157	1.5085	1.3945
B3LYP/cc-pvdz	-350.2156098	1.5115	1.4025

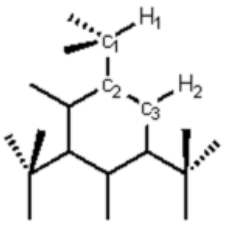

Table 2.
Comparison of calculation with experimental data of vibr ations of 1,3,5-trimethylbenzene.

6b	516	557	556	523	523	525	522
1	579	611	608	579	577	578	580
9a	935	1017	1012	956	951	950	948
8a	1613	1808	1796	1663	1650	1646	1654
2	3020	3350	3328	3171	3150	3153	3159

1 : HF/6-31g*, 2 : HF/6-311g*, 3 : B3LYP/6-31g*, 4 : B3LYP/6-311g*, 5 : B3LYP/6-31g(df,pd), 6 : B3LYP/cc-pvdz

□.2 The $D_1 \rightarrow D_0$ spectra of 3,5-dimethylbenzyl radical

The weak visible emission spectrum of 3,5-dimethylbenzyl radical is believed to arise from transitions from the close-lying 2^2B_2 and 1^2A_2 excited states to the 1^2B_2 ground state like benzyl raidcal. Two excited electronic states are mixed through vibronic coupling. Ring substitution is also expected to affect the energies of the 2^2B_2 and 1^2A_2 excited states differently. The transition from the second excited state to the ground state has not been observed due to the rapid collisional relaxation process.

Figure 5 exhibits a portion of the vibronic emission spectrum of the 3,5- dimethylbenzyl radical generated in this work. Most of the bands are observed in the region of 18500-21500 cm^{-1}. As shown in Figure 6, the spectrum exhibits one kind of bandshape. The strong band at 20842 cm^{-1} shows the bandshape of Figure 6(a) and also the other strong band 20332 cm^{-1} represent the same character in the spectrum.

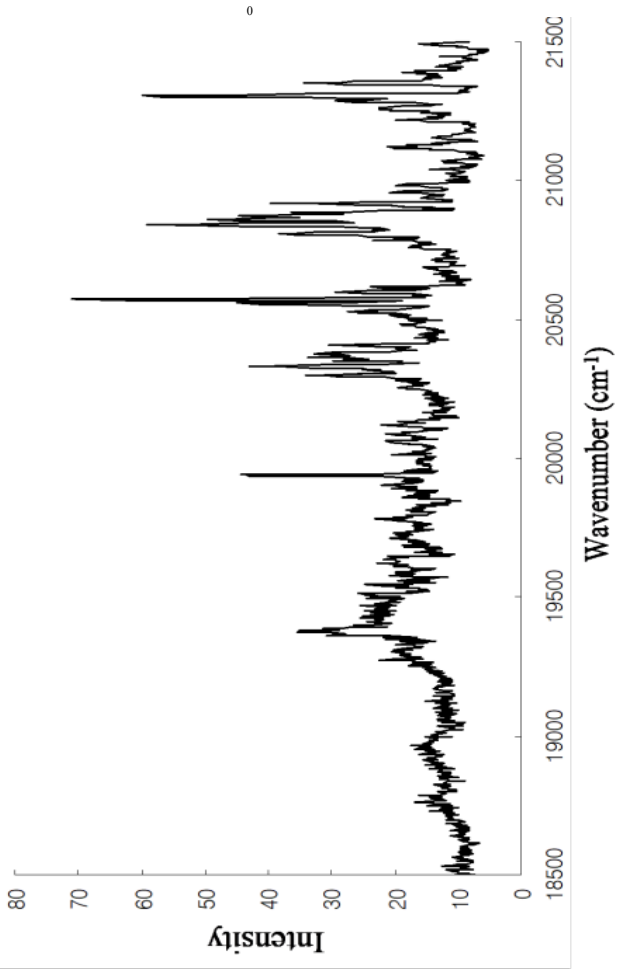

Figure. 5. Vibronic emission spectrum of the 3,5-dimethylbenzyl radical.

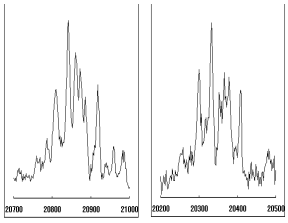

Figure. 6. Enlarged bandshape of 3,5-dimethylbenzyl radical.

In the spectrum, the most intensive band is found at 20842

cm^{-1} which is believed to be the origin band of the $D_1(1^2A_2) \rightarrow D_0(1^2B_2)$ transition, followed to lowed energies by a series of vibronic band. It also seems that *o*-, *m*-, and *p*-methyl-substitution affect independently the energy of the benzyl radical. For example, 3,5-dimethylbenzyl radical has two substituted methyl group of meta. So like the prediction of 2,4,5-trimethylbenzyl radical, we would predict the energy of origin of 3,5-dimethylbenzyl radical like 22002 - (2 × 517) = 20968 cm^{-1}. It can be comparable with experimental data, 20842 cm^{-1}. Moreover, the substitution effect is proved by comparing other methylbenzyl radical. In Figure 7, the 3,5-dimethylbenzyl radical is similar with *m*-xylyl radical but not *o*- or *p*- xylyl radical. It means that 3,5-dimethylbenzyl radical spectrum is influenced by two meta methyl groups.

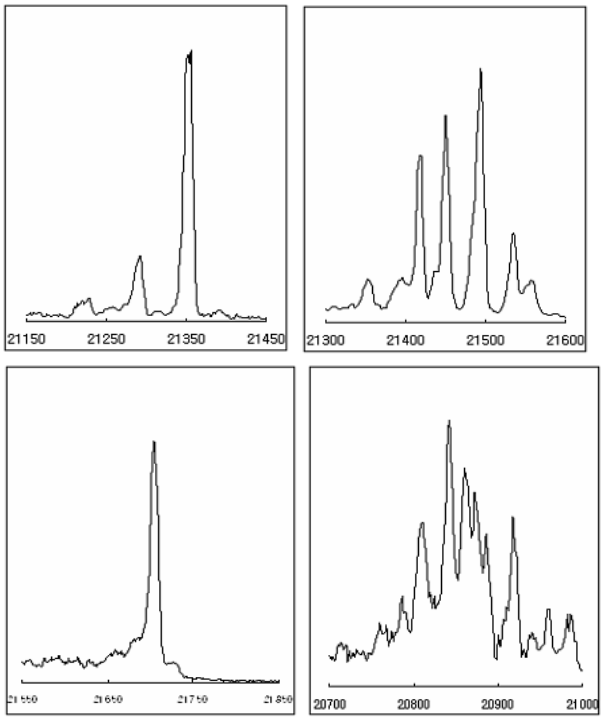

Figure. 7. Enlarged origin bandshape of mono-substituted methylbenzyl radical with 3,5-dimethylbenzyl radical.

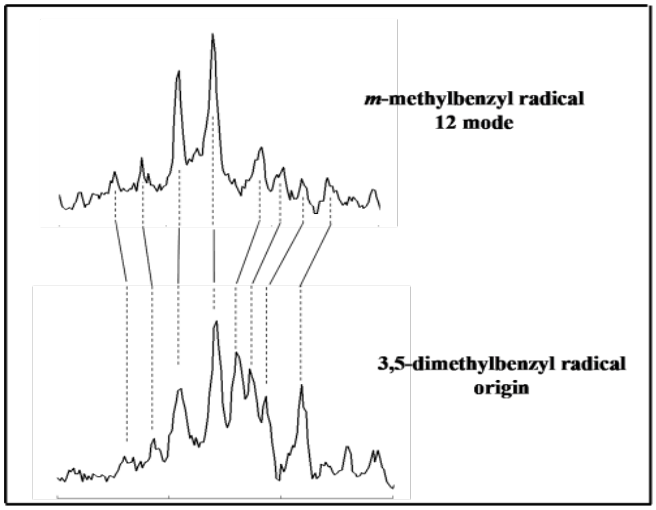

Figure. 7-1. Comparison of vibronic 12 band of *m*-methylbenzyl radical with origin band of 3,5-dimethylbenzyl radical.

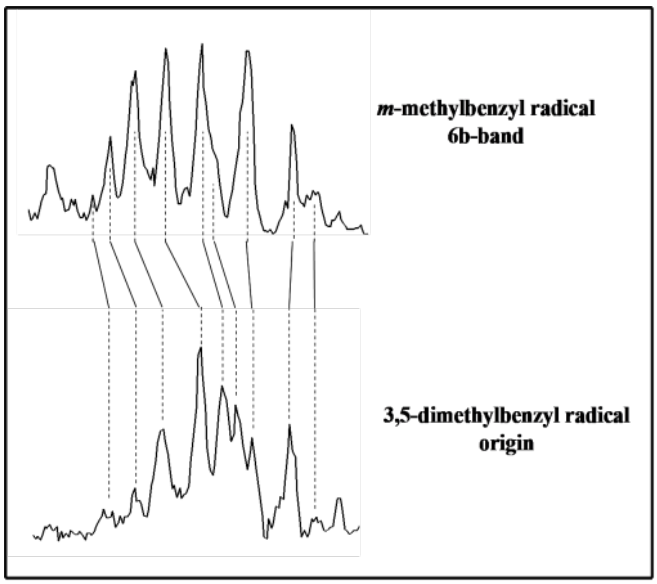

Figure. 7-2. Comparison of vibronic 12 band of *m*-ethylbenzyl radical with origin of 3,5-dimethylbenzyl radical.

The vibronic bands observed in this work were provisionally assigned with the help of the known vibrational mode frequencies of the precursor, 1,3,5-trimethylbenzene since both molecules are subjected to the isodynamic approximation which states the correspondence of vibrational mode frequencies and intensity.

It has been also accepted that the calculation using GAUSSIAN 09 program calculation method predicts the vibrational mode frequencies within +10% from the experimental values. From the calculation on the 3,5-dimethylbenzyl radical, a total of 54 vibrational mode frequencies have been obtained.

Table 3 lists the frequencies of the transitions observed, together with the relative intensities of the peaks measured in this work and Table 11 shows the comparison of calculation with precursor data. The numbers in the parenthesis represent the spacing from the origin band in units of wavenumber. The strong band at 20332(510) cm^{-1} was assigned to the 6a transition according to the similarity to the precursor (516 cm^{-1}). The slight discrepancy from the precursor reflects the change of $-CH_3$ to $-CH_2$.

In the vibronic emission spectrum of benzyl-type radicals with C_{2v} symmetry, the mode 6a of ring deformation was observable with fairly strong intensity while the mode 6b was detected with much weak intensity. In m-methylbenzyl radical, the frequency of modes 6a and 6b was measured to be 538 and 506 cm^{-1} respectively.

The calculation value supports the 6a mode in the Table 4 moreover, as shown in Figure 9, the band of mode 6a also exhibits the similar bandshape with the origin band, indicating that the vibrational mode comes from 3,5-dimethylbenzyl radical.

Although the several weak bands observed in this work and the peaks may be the combination bands and overtone transitions, but we exclude to assign these bands to the other vibrational modes. Because it does not have enough proofs to explain vibrational mode like a bandshape and peaks of 21308 and 20574 cm^{-1} are CH-fragment. These peaks are observed every methyl-substituted toluene discharge.

Table 10. List of the vibronic bands observed and their assignment of 3,5-dimethylbenzyl radical.

position	relative intensity	spacing from the origin	assignment
20842	s	0	origin
20574	s	268	CH-fragment
20332	m	510	0_1^1 6a
19940	m	900	He

Table 11. Comparison of calculation with precursor data of vibronic bands of ,3,5-dimethylbenzyl radical.

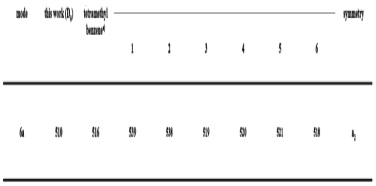

1 : HF/6-31g*
2 : HF/6-311g*
3 : B3LYP/6-31g*
4 : B3LYP/6-311g*
5 : B3LYP/6-31g(df,pd)

IV. CONCLUSION

The vibronically cooled electronic emission spectra of the trimethyl- and dimethylbenzyl radical was observed in a corona excited supersonic expansion apparatus. Several fundamental modes 1, 3, 5- trimethylbenzyl and 3, 5-dimethylbenzyl were assigned on the basis of previous infrared and Raman values of the precursor and calculation. The spectrum was analyzed in terms of progressions of the fundamental vibrational modes and molecular structures of benzene, toluene and methyl-substituted toluene are calculated and compared with experimental data.

We have generated for the first time the 1, 3, 5-trimethylbenzyl radical, 3,5-dimethylbenzyl radical in a jet from which the vibronic emission spectra in the $D_1 \rightarrow D_0$ transition have been recorded.

In the D_0 electronic state, we assigned several vibrations by comparison with frequency calculations of HF and B3LYP and with the gas-phase IR absorption data of the precursor. The measured D_0 vibrational frequencies matched the calculated method frequencies to within 5% using B3LYP method. The calculation method, Density Function Theory make better result than HF method. DFT is profitable to predict molecular frequencies and structure.

References

[1] J. C. Whitehead, Rep. Prog. Phys. **1996,** 59, 993.
[2] R. S. Mulliken, Phys. Rev. **1927,** 30, 785.
[3] W. E. Pretty, Proc. Phys. Soc. **1928,** 40, 71.
[4] F. Hund, **1926,** 36, 657.
[5] F. Paneth and W. Hofeditz, Ber. Chem. Ges. **1929,** 62, 1335.
[6] F. O. Rice, J. Am. Chem. Soc. **1931,** 53, 1959.
[7] G. Herzberg, The Spectra and Structure of Simple Free Radicals. (Cornell University Press, Ithaca, NY, 1971).
[8] J. I. Selco, P. G. Carrick, J. Mol. Spectrosc. **1989,** 137, 13.
[9] C. Cossart-Magos, S. Leach, J. Chem. Phys. **1976,** 64, 4006.
[10] T.F. Bindley, A.T. Watts, S. Walker, Trans. Faraday Soc. **1964,** 60, 1.
[11] M. Fukushima, K. Obi, J. Chem. Phys. Lett. **1990,** 93, 8488.
[12] T.-Y. Lin, X.-Q. Tan, T.M. Cerny, J.M. Williamson, D.W. Cullin, T.A. Miller, Chem. Phys. **1992,** 167, 203.
[13]S. K. Lee, S. Y. Chae, J. Phy. Chem. A. **2002,** 106, 8054.
[14]S. K. Lee, S. Y. Chae, J. Phy. Chem. A. **2001,** 105, 5808.
[15] S.K. Lee, D.Y. Baek, Chem. Phys. Lett. **1999,** 304, 39.
[16] S.K. Lee, S. J. Kim, Chem. Phys. Lett. **2005,** 41,2 88.
[17] S.K. Lee, S.K. Lee, J. Phys. Chem. A. **2001,** 105, 3034.
[18] S.K. Lee, D. Y. Baek Chem. Phys. Lett. **1999,** 30,1 407.
[19] S.K. Lee, D.Y. Baek, Chem. Phys. Lett. **1999,** 301, 407.
[20] S.K. Lee, D.Y. Baek, J. Phys. Chem. A. **2000,** 104, 5219.
[21] S.K. Lee, D.Y. Baek, Chem. Phys. Lett. **1999,** 31,1 36.
[22] M.H. Suh, S.K. Lee, T.A. Miller, J. Mol. Spectrosc. **1999,** 194, 211.
[23] G.W. Lee, S.K. Lee, J. Phys. Chem. A. **2006,** 110, 2130.
[24] G. W. Lee, S.K. Lee J. Phys. Chem. A. **2007,** 111, 6003.
[25] G. W. Lee, S.K. Lee, Chem. Phys. Lett, **2005,** 410 6.

Chang Soon Huh, Assistant Professor

Applied Chemistry Major, Division of Chemical and Environmental Engineering, College of Engineering, Dong-eui University, 176 Eomgwangno, Busanjin-gu, Busan, 47340, South Korea

Tel: +82-51-890-1518
C/P: +82-10-4590-8481